

## Finite Differences Example

The following solution of the simple planar potential flow around a right-angled corner will help illustrate the finite difference method for a flow governed by an elliptic partial differential equation. A sketch of the flow is presented in Figure 1 and we have chosen to construct within the flow a rectangular grid with a uniform spacing that we will denote by  $h$ . Of course, most engineering flows have much more complicated, non-rectangular boundaries and may need grids with a finer mesh in some parts of the flow. But such complexities can be treated later when the basic methodology has been established. The interior grid

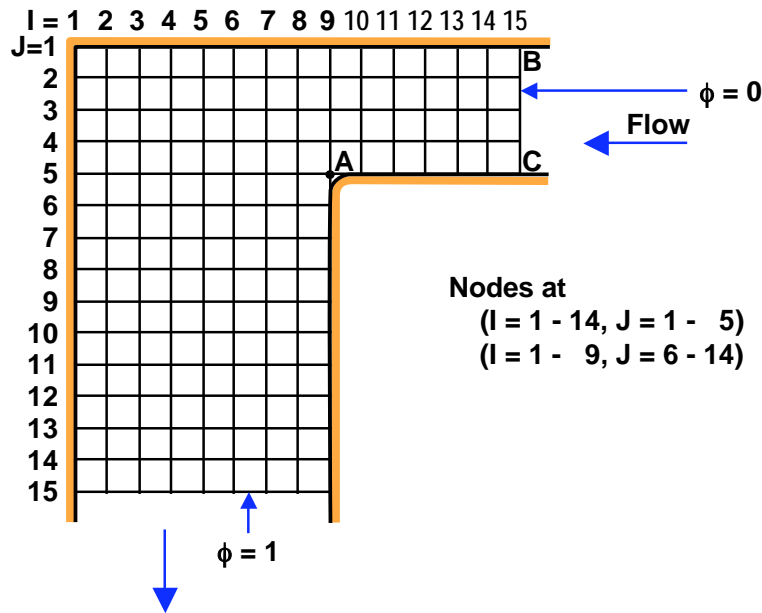


Figure 1: Mesh grid and notation for the flow around a corner.

points ( $I = 2$  to  $8$ ,  $J = 2$  to  $14$ , and  $I = 9$  to  $14$ ,  $J = 2$  to  $4$ ) and the solid boundary grid points ( $I = 1$ ,  $J = 1$  to  $14$  and  $I = 9$ ,  $J = 7$  to  $14$  and  $J = 1$ ,  $I = 1$  to  $14$  and  $J = 5$ ,  $I = 11$  to  $14$ ) will be treated as described in the previous section. The inlet boundary ( $I = 15$ ) and the discharge boundary ( $J = 15$ ) will also be treated as previously described. We choose to assign a value of  $\phi = 0$  to the inlet boundary ( $I = 15$ ,  $J = 1$  to  $5$ ) since the velocity potential always has one constant that can be arbitrarily selected. We choose to assign a value of  $\phi = 1$  to the discharge boundary ( $J = 15$ ,  $I = 1$  to  $9$ ) for the following reason: since the equations governing the flow field are homogeneous in the velocity potential we could multiply all the solution values of  $\phi$  by a uniform constant and the result would still satisfy all those equations. In practice we might wish to stipulate a certain volume-averaged velocity at the inlet. If so then we could calculate from the solution what that volume-averaged velocity is for the scaling implicit in the choice of the discharge surface  $\phi$  and then scale all the  $\phi$  values up or down in order to match the stipulated volume-averaged velocity.

In the solution presented below we have chosen to avoid the issue of the singular behavior at the projecting corner  $A$  in Figure 1 by essentially rounding off the corner and not attempting to solve for the details of the flow in that region. However, it is valuable to describe how this singular point might be more accurately treated. To do so we note first from the solutions detailed in the section on the method of complex variables for planar potential flows that the form of the velocity potential for the flow close to a

projecting 90° corner is  $\phi = \phi'$  where

$$\phi' = \phi_0 + C^* r^{\frac{2}{3}} \cos(2\theta/3) \quad (\text{Od1})$$

where  $\phi_0$  is the value at the vertex,  $C^*$  is the magnitude of the singular behavior at the vertex and the polar coordinates  $(r, \theta)$  are based on the vertex  $A$  with  $\theta = 0$  being in the  $x$  direction. It follows that if the grid points in the immediate neighborhood of the vertex  $A$  were to adhere precisely to this form then:

$$\phi'_{9,5} = \phi_0 \quad ; \quad \phi'_{10,5} = \phi_0 + C \quad ; \quad \phi'_{9,4} = \phi_0 + \frac{C}{2} \quad ; \quad \phi'_{8,5} = \phi_0 - \frac{C}{2} \quad ; \quad \phi'_{9,6} = \phi_0 - C \quad (\text{Od2})$$

where  $C = C^* h^{2/3}$ . The normal finite difference strategy for treating a singular point such as  $A$  at which some of the derivatives become infinite and therefore the Taylor series expansion breaks down is to consider the velocity potential to be the sum of a singular velocity potential,  $\phi'$ , and a regular component,  $\Delta\phi$ , which is well-behaved. Then the numerical strategy is to identify the form of the singularity, use the numerical values at surrounding nodes to estimate the strength of the singularity and to treat the regular component as one would elsewhere in the flow field. In the present example we note that the equations (Od2) mean that

$$\phi'_{10,5} + \phi'_{9,4} + \phi'_{8,5} + \phi'_{9,6} - 4\phi'_{9,5} = 0 \quad (\text{Od3})$$

and therefore, somewhat unusually, the singular component satisfies the same numerical relation, equation (Oc9), at the vertex as we seek to satisfy at all the other nodes and as we wish the regular component,  $\Delta\phi$ , to satisfy. Consequently, it is not necessary to treat the vertex  $A$  any differently than any other grid point. If we wish to go one step further we could use somewhat improved finite difference equations at the nodes (10, 5), (9, 4), (8, 5), and (9, 6). For example, at the grid point (10, 5) we might use  $(\phi_{11,5} - \phi_{10,5})/h$  for  $(\partial\phi/\partial x)$  midway between points (11, 5) and (10, 5) but instead of  $(\phi_{10,5} - \phi_{9,5})/h$  for  $(\partial\phi/\partial x)$  midway between points (10, 5) and (9, 5) (which would be inaccurate because of the singular behavior at (9, 5)) we might use  $0.84(\phi_{10,5} - \phi_{9,5})/h$  which would be consistent with the singular behavior identified above. It would then follow that a more accurate finite difference form for  $(\partial^2\phi/\partial x^2)$  at the grid point (10, 5) would be

$$\left\{ \frac{\partial^2\phi}{\partial x^2} \right\}_{10,5} = \frac{1}{h} \left\{ \frac{\phi_{11,5} - \phi_{10,5}}{h} - \frac{0.84(\phi_{11,5} - \phi_{10,5})}{h} \right\} = \frac{1}{h^2} \{ \phi_{11,5} + 0.84\phi_{9,5} - 1.84\phi_{10,5} \} \quad (\text{Od4})$$

An analogous treatment should then be used at the grid points (9, 4), (8, 5), and (9, 6). In addition modified finite difference formulae should be used in evaluating the first derivatives and therefore the velocities and pressures at the midpoints between grid point (9, 5) and the surrounding grid points (10, 5), (9, 4), (8, 5), and (9, 6). However, for simplicity, no special treatment was applied in obtaining the numbers which follow.

Converged values for  $\phi$  at each of the grid points for the "unit" problem with  $\phi = 0$  at inlet and  $\phi = 1$  at outlet are shown in Figure 2. Note that despite the lack of any special treatment in the neighborhood of the vertex  $A$  the solution near that point adheres quite closely to the features listed in equation (Od2). The next step is to evaluate the flow rate in, calculate the volume-averaged velocity and scale the results so that the volume-averaged velocity is unity. To do this we first evaluate the fluid velocities inherent in "unit" solution. Velocities are best evaluated at the midpoints between the grid points and the velocities in the  $x$  direction at inlet are therefore evaluated midway between the grid points (14,  $J$ ) and (15,  $J$ ) (for  $J = 1 \rightarrow 5$ ). Denoting these velocities by  $u_{inlet}^J$ :

$$u_{inlet}^J = \frac{(\phi_{14,J} - \phi_{15,J})}{h} \quad \text{for} \quad J = 1 \rightarrow 5 \quad (\text{Od5})$$

and therefore the volume flow rate in per unit depth normal to the plane of the flow,  $\dot{V}$  is given by numerically integrating these velocities across the inlet so that, using Simpson's rule,

$$\dot{V} = \frac{h}{2} \{ u_{inlet}^1 + 2u_{inlet}^2 + 2u_{inlet}^3 + 2u_{inlet}^4 + u_{inlet}^5 \} \quad (\text{Od6})$$

	<b>I = 1</b>	<b>2</b>	<b>3</b>	<b>4</b>	<b>5</b>	<b>6</b>	<b>7</b>	<b>8</b>	<b>9</b>	<b>10</b>	<b>11</b>	<b>12</b>	<b>13</b>	<b>14</b>	<b>15</b>
<b>J = 1</b>	0.6314	0.6285	0.6197	0.6048	0.5832	0.5543	0.5174	0.4718	0.4174	0.3554	0.2882	0.2179	0.1459	0.0731	0.0000
<b>2</b>	0.6342	0.6314	0.6228	0.6081	0.5869	0.5583	0.5217	0.4761	0.4212	0.3581	0.2898	0.2187	0.1463	0.0733	0.0000
<b>3</b>	0.6428	0.6401	0.6319	0.6180	0.5978	0.5705	0.5350	0.4898	0.4333	0.3658	0.2941	0.2209	0.1474	0.0737	0.0000
<b>4</b>	0.6568	0.6543	0.6469	0.6342	0.6157	0.5908	0.5580	0.5147	0.4563	0.3779	0.2998	0.2235	0.1485	0.0741	0.0000
<b>5</b>	0.6757	0.6735	0.6670	0.6560	0.6402	0.6191	0.5916	0.5547	0.4994	0.3897	0.3035	0.2249	0.1491	0.0743	0.0000
<b>6</b>	0.6989	0.6971	0.6917	0.6826	0.6700	0.6538	0.6344	0.6133	0.5968						
<b>7</b>	0.7257	0.7242	0.7199	0.7129	0.7033	0.6917	0.6790	0.6673	0.6611						
<b>8</b>	0.7553	0.7542	0.7510	0.7457	0.7388	0.7307	0.7225	0.7158	0.7129						
<b>9</b>	0.7872	0.7864	0.7840	0.7802	0.7753	0.7698	0.7645	0.7605	0.7590						
<b>10</b>	0.8207	0.8202	0.8184	0.8157	0.8124	0.8087	0.8053	0.8028	0.8019						
<b>11</b>	0.8555	0.8550	0.8539	0.8520	0.8497	0.8473	0.8451	0.8436	0.8430						
<b>12</b>	0.8910	0.8907	0.8899	0.8887	0.8872	0.8857	0.8843	0.8834	0.8830						
<b>13</b>	0.9270	0.9269	0.9264	0.9257	0.9248	0.9239	0.9231	0.9225	0.9223						
<b>14</b>	0.9634	0.9634	0.9631	0.9628	0.9624	0.9620	0.9616	0.9613	0.9613						
<b>15</b>	1.0000	1.0000	1.0000	1.0000	1.0000	1.0000	1.0000	1.0000	1.0000						

Figure 2: Solution values for the velocity potential,  $\phi$ .

and the volume-averaged velocity,  $U$ , is therefore  $U = \dot{V}/4h$ . Hence the velocities components scaled by the volume-averaged inlet velocity are given at points midway between the grid points by

$$u_{I+\frac{1}{2},J} = \frac{4(\phi_{I,J} - \phi_{I+1,J})}{\dot{V}} \quad \text{and} \quad v_{I,J+\frac{1}{2}} = \frac{4(\phi_{I,J+1} - \phi_{I,J})}{\dot{V}} \quad (\text{Od7})$$

where  $u$  is positive to the left and  $v$  is positive downward. The scaled velocities at the walls are presented in Figure 3. In addition scaled velocity vectors and streamlines constructed to be everywhere tangential

	<b>I = 1</b>	<b>2</b>	<b>3</b>	<b>4</b>	<b>5</b>	<b>6</b>	<b>7</b>	<b>8</b>	<b>9</b>	<b>10</b>	<b>11</b>	<b>12</b>	<b>13</b>	<b>14</b>	<b>15</b>
<b>J = 1</b>		0.0392	0.1189	0.2025	0.2927	0.3918	0.5011	0.6188	0.7372	0.8406	0.9118	0.9539	0.9764	0.9875	0.9920
<b>2</b>	0.0392														
<b>3</b>	0.1163														
<b>4</b>	0.1894														
<b>5</b>	0.2563									1.4881	1.1686	1.0663	1.0288	1.0139	1.0085
<b>6</b>	0.3147							1.3211							
<b>7</b>	0.3635							0.8723							
<b>8</b>	0.4025							0.7034							
<b>9</b>	0.4325							0.6249							
<b>10</b>	0.4547							0.5825							
<b>11</b>	0.4708							0.5577							
<b>12</b>	0.4819							0.5425							
<b>13</b>	0.4893							0.5333							
<b>14</b>	0.4938							0.5280							
<b>15</b>	0.4959							0.5255							

Figure 3: Solution values for the scaled velocities at midpoints on the walls.

to the velocity vectors are shown in Figure 4. Note the large velocities in the vicinity of the projecting vertex,  $A$ .

Finally the pressure coefficient,  $C_P$ , can be calculate from the definition

$$C_P = \frac{p - p_{14+\frac{1}{2},5}}{\frac{1}{2}\rho U^2} \quad (\text{Od8})$$

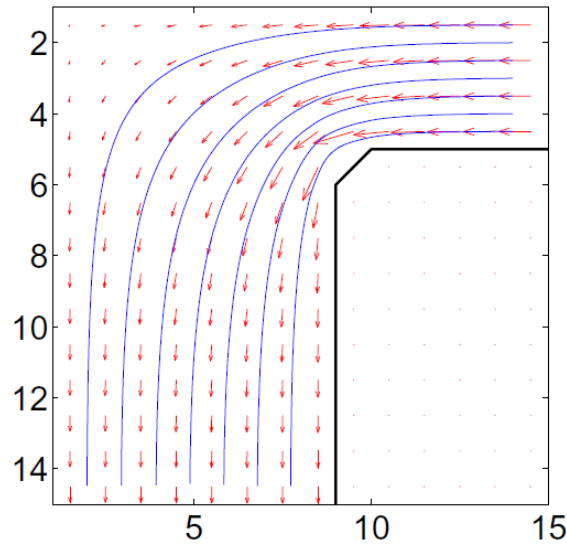


Figure 4: Flow vectors and streamlines.

where we have arbitrarily used the grid point  $(14 + \frac{1}{2}, 5)$  as the pressure reference point. From Bernoulli's equation

$$p + \frac{1}{2}\rho(u^2 + v^2) = p_{14+\frac{1}{2},5} + \frac{1}{2}\rho u_{14+\frac{1}{2},5}^2 \quad (\text{Od9})$$

and therefore

$$C_P = \frac{u_{14+\frac{1}{2},5}^2 - (u^2 + v^2)}{U^2} \quad (\text{Od10})$$

Values of the pressure coefficients on the walls at the midpoints are shown in Figure 5.

<b>I = 1</b>	<b>2</b>	<b>3</b>	<b>4</b>	<b>5</b>	<b>6</b>	<b>7</b>	<b>8</b>	<b>9</b>	<b>10</b>	<b>11</b>	<b>12</b>	<b>13</b>	<b>14</b>	<b>15</b>
<b>J = 1</b>	1.0155	1.0029	0.9760	0.9314	0.8635	0.7659	0.6341	0.4736	0.3104	0.1856	0.1071	0.0636	0.0419	0.0331
<b>2</b>	1.0155													
<b>3</b>	1.0035													
<b>4</b>	0.9812													
<b>5</b>	0.9514							-1.1975	-0.3486	-0.1200	-0.0413	-0.0109	0.0000	
<b>6</b>	0.9180						-0.7282							
<b>7</b>	0.8849						0.2561							
<b>8</b>	0.8550						0.5223							
<b>9</b>	0.8300						0.6266							
<b>10</b>	0.8102						0.6777							
<b>11</b>	0.7954						0.7061							
<b>12</b>	0.7848						0.7227							
<b>13</b>	0.7776						0.7327							
<b>14</b>	0.7732						0.7383							
<b>15</b>	0.7711						0.7409							

Figure 5: Solution values for the pressure coefficient at midpoints on the walls.